Reaction Kinetics, Mechanisms and Catalysis (2020) 129:471–490
https://doi.org/10.1007/s11144-019-01716-4

ZSM-5 zeolites modified with Zn and their effect on the crystal size in the conversion of methanol to light aromatics (MTA)

Misael García Ruiz, et al. ***[full author details at the end of the article]***

Received: 17 October 2019 / Accepted: 21 December 2019 / Published online: 2 January 2020

Abstract

ZSM-5 zeolite catalysts modified with zinc were prepared by two forms of Zn incorporation the synthesis gel, and ion exchange techniques. The physico-chemical properties of zeolites were studied by XRD, N_2-adsorption, NH_3 temperature-programmed desorption, ^{27}Al and ^{29}Si MAS NMR, SEM, TEM and TGA. ZSM-5 zeolite in its acid form was exchanged using an aqueous zinc salt solution and demonstrated a significantly higher selectivity for the aromatic products in comparison with the purely acidic catalysts. The samples with distribution of $ZnOH^+$ species are more active than the samples with ZnO sites in the zeolites. The synthesis of zeolite ZSM-5 of nanometric size resulted to present high stability and selectivity towards light aromatics. The influence of the form of zinc incorporation, the acidity and the reaction temperature had a great influence on the catalytic activity. The MTA catalyst lifetime is increased by several times due to the enhanced mesoporosity and decreased acidity. In the present work the zeolite HZSM-5 exchanged with Zn with Si/Al 25 ratio presented conversions close to 100% methanol with 32% selectivity to the BTX fraction, however, this catalyst was deactivated after 8 h of reaction with a weight hourly space velocity of 4.74 h^{-1} at 450 °C. On the other hand, a HZSM-5 zeolite with nanoscale crystals was found to be more stable in the MTA reaction. The nanometric catalyst showed conversions around 100% methanol after 8 h of reaction and 32.5% selectivity to the BTX fraction to 450 °C. These results clearly indicate that crystal size significantly influence the ZSM-5 lifetime and product distribution.

Keywords ZSM-5 zeolite · MTA process · BTX fraction · Modified zeolites · Nanocrystalline zeolite

Electronic supplementary material The online version of this article (https://doi.org/10.1007/s11144-019-01716-4) contains supplementary material, which is available to authorized users.

Introduction

Aromatic compounds, especially benzene, toluene and xylenes (BTX) are important chemical compounds conventionally obtained from raw materials based on crude oil. Currently, more than 90% of these aromatic compounds are obtained by reforming different petroleum fractions and subsequent stages of treatment, purification or modification of the aromatic mixture are necessary to obtain the most desired compounds, such as the para-xylene, which, obviously, makes the process even more expensive [1]. In the last decade, the route of methanol conversion to aromatics (MTA) has received great attention considering that methanol is readily available from general resources such as coal, natural gas or biomass [2].

Zeolites are crystalline metallosilicates containing ordered micropores that enable shape-selective transformation. Given the high thermal stability and strong Brønsted acidity of zeolite catalysts, they are widely used in cracking, disproportionation, isomerization, alkylation, and aromatization [3–6]. The aromatization reaction has been observed with a range the active metal species in zeolites include Zn, La, Ga, Ag, Cu, Sn, Ni, Mo and Cr, however, the selectivity to a specific product versus time is different in each case. Furthermore, it has been widely accepted that Zn species could greatly increase the selectivity of BTX in MTA reaction compared with other metal species. Inoue et al. [7] reported that an Ag/ZSM-5 catalyst the products contain too much heavy aromatics and the stability is poor. The aromatization performance of methanol over Mo_2C/ZSM-5 was also investigated for Barthos et al. [8], and it was found that the loading of Mo_2C enhanced the formation of aromatics enormously. Nevertheless, in this process there exist difficulties for controlling the exothermicity of the reaction and for decreasing the rapid rate of catalyst deactivation. Therefore, the main challenge of our work is to improve the lifetime of the catalyst, because in previous reports the ZMS-5 zeolite is deactivated in relatively short reaction times. In this context, nanosized zeolites with a considerable amount of fully accessible acid sites located on the external surface may be potentially interesting catalysts for methanol reactions.

ZSM-5 zeolite has proved to be the most promising component of aromatization catalyst because of its hydrothermal stability, shape-selective behavior, and proper crystal structure for high activity [9–11]. As demonstrated in previous studies [12], certain medium pore zeolites (with 10-membered channels) such as ZSM-5, doped with Zn is capable of transforming methanol into aromatic compounds, presenting high selectivities to the BTX fraction. In this case, Zn-containing zeolites are usually synthesized by traditional techniques such as ion exchange (i) or in the synthesis gel (G) [13]. Pan et al. [14] demonstrated that the Zn introduction method had obvious influences on texture properties, acidic properties and subsequent influences on catalytic activity. The BTX selectivity was effectively improved by introduction of Zn species in ion exchange, owing to the enhancement of Zn-based acid sites with increased density to aromatization of intermediates in MTA reaction. On the contrary, zinc in synthesis gel produce ZnO clusters at the pore entrances might restrict large molecule products diffusion and deteriorated the catalyst deactivation.

The zeolite ZSM-5 of nanometric size has a long catalytic life, due to the fact that the reduction of the size of crystal shortens the length of diffusion of molecules, making the zeolite more stable and increasing the selectivity to the BTX fraction [15]. The catalysts were prepared by the ion exchange of ZSM-5 zeolite (acid-form) with aqueous solution of zinc salts and demonstrated significantly higher selectivity for aromatics compared to the catalysts on pure acid-form ZSM-5 zeolite [13]. Although some significant achievements have been made in recent years, it is necessary to further improve the activity and stability of the catalyst in the MTA reaction [3–6]. For this, the relationship between the properties of the catalyst and its behaviour in the reaction has been studied in order to be able to develop a more efficient catalyst. Therefore, in the present work the study of zeolitic catalysts with different forms of Zn incorporation is proposed, realizing a comparison between the catalytic behaviour of nanocrystalline and microcrystalline ZSM-5 samples for MTA reaction, improving the resistance to the deactivation of the catalysts.

Experimental

Materials

The reagents used for the preparation of ZSM-5 zeolites are tetraethyl orthosilicate (TEOS, 98%, Aldrich), fumed silica, sodium hydroxide (NaOH), sodium aluminate (41 wt% Al_2O_3, 37 wt% Na_2O), the cationic template (1 M TPAOH, Acros Organics, 8 mL), tetrapropyl ammonium bromide (TPABr 98 wt%), ethanol absolute, for HPLC, ≥ 99.8% (Sigma-Aldrich) and zinc nitrate hexahydrate ($Zn(NO_3)_2{\cdot}6H_2O$ reagent grade, 98%, Sigma-Aldrich).

ZSM-5 by hydrothermal synthesis

HZSM-5 zeolites were synthesized for hydrothermal method with a molar ratio of $xSiO_2$–yAl_2O_3–0.2TPABr–0.09Na_2O–35H_2O, where x/y represents the Si/Al molar ratio of 25. In a conventional synthesis, sodium aluminate and sodium hydroxide were dissolved in deionized water, and once dissolved, tetrapropyl ammonium bromide (TPABr) was added as structure directing agent (SDA). Finally, fumed silica was added as the silica source and the gel was stirred for one hour. The synthesis gel was placed in stainless steel autoclaves with Teflon sheath, at 160 °C under static conditions for 72 h. The solid was recovered by filtration, dried at 70 °C, ground and calcined at 550 °C for 8 h in an air atmosphere. The H-type ZSM-5 (H-ZSM-5) samples were obtained as follows. The calcined Na-ZSM-5 samples It was exchanged with a solution 1 M NH_4NO_3 at 80 °C for 4 h followed by calcination at 550 °C for 6 h to exchange Na^+ ions for proton. The acid zeolites with a Si/Al molar ratio of 25 was denoted as HZ25. Zeolite modified with Zn in synthesis gel (G) was synthetized under similar conditions as the previous zeolite, except, in the first step sodium aluminate and sodium hydroxide were dissolved and $Zn(NO_3)_2{\bullet}6H_2O$ as a source of zinc was added. The molar relation was

$xSiO_2$–yAl_2O_3–0.2TPABr–0.09Na_2O–zZnO–35H_2O, where x/y represents the molar ratio Si/Al (50) and z represents the amount of zinc. Similar in conventional synthesis. The material was denoted as HZ50 0.01 Zn-G.

Synthesis of nanocrystalline ZSM-5 zeolite

Nano-ZSM-5 zeolites with an average crystal size of 60 nm [16] and ratio Si/Al 25 and 50 were synthesized from a gel mixture with a final molar composition: xTEOS–$NaAlO_2$–5TPAOH–4TPABr–1000H_2O. First, the sodium aluminate was dissolved in deionized water, the TPABr was added and stirred until was completely dissolved. Then the TPAOH was added to the synthesis gel. TEOS was added dropwise to the reaction mixture which was stirred overnight at room temperature. The reaction mixture was evaporated at 60 °C until 20% of the total volume amount of the mixture evaporated.

The reaction solution was placed in a stainless-steel autoclave. The synthesis was carried out with constant agitation at 250 rpm at 160 °C for 72 h. After the synthesis, the zeolite crystals were separated by centrifugation at 14,000 rpm for 20 min. 100 mL ethanol was added to the solid and the resulting suspension was subjected to a sonication process for 1 h, the crystals were again separated by centrifugation at 14,000 rpm for 20 min. The solid was redispersed by sonication in water for 1 h, the solid was separated by centrifugation, dried at 70° C and calcined at 550° C for 6 h with air flow. The Na-ZSM-5 zeolite is exchanged with a 1 M solution at 80 °C for 4 h, the solid is filtered, dried and calcined at 550° C for 4 h in air. This acid catalyst was denoted as nano HZ25.

Synthesis of HZSM-5 zeolites exchanged with Zn

The acid zeolites previously synthesized (H-ZSM-5) was exchanged with a 0.025 M solution of $Zn(NO_3)_2{\cdot}6H_2O$ at 80 °C for one night. The zeolite was filtered, washed and dried at 70° C, finally the resulting powder was calcined at 550 °C for 4 h with air flow. The zeolites synthesized by hydrotreatment with ratio Si/Al 25 was denoted as HZnZ25-i. The nanocrystalline zeolite with zinc was denoted as nano HZnZ25-i.

Catalyst characterization

X-ray diffraction of powders (XRD) was collected with an XPert Pro PANalytical diffractometer (CuKα1 radiation = 0.15406 nm). Scanning electron microscopy (SEM) images were recorded on a Hitachi S-3000N microscope. Transmission electron microscopy (TEM) study was carried on a JEOL 2100F microscope operating to 200 KV. Nitrogen adsorption/desorption isotherms were measured at − 196 °C in a Micromeritics ASAP 2020 device. Before the measurement, calcined samples were degassed out at 350 °C under high vacuum for at least 10 h. Surface areas were measured by using the Brunauer–Emmet–Teller (BET) equation, whereas microporous and external surface areas were estimated by applying the t-plot method.

Solid-state magic-angle spinning (MAS) NMR experiments were conducted on a Brucker AV 400WB spectrometer operated with frequency at 79.5 MHz and spinning rate at 10 kHz. The ^{27}Al NMR spectra were recorded using a pulse width of 0.5 μs (π/12 flip angle), 2400 scans and a recycle delay of 1 s.

The Al and Si concentrations of samples were obtained by inductively coupled plasma-optical emission spectroscopy (ICP-OES) with a Optima 3300 DV Perkin Elmer. Ammonia Temperature programmed desorption (NH_3-TPD) was acquiered using a Micrometrics Autochem II chemisorption analysis equipment. Typically, 100 mg of sample pellets (30–40 mesh) were pretreated at 550 °C for 1 h in helium flow (25 mL min^{-1}) and then cooled to the adsorption temperature (177 °C). A gas mixture of 5.0 vol% NH_3 in He was then allowed to flow over the sample for 4 h at a rate of 15 mL min^{-1}. Afterwards, samples were flushed with a 25 mL min^{-1} helium flow for 30 min while maintaining the temperature at 177 °C to remove weakly adsorbed NH_3, and finally the temperature was increased to 550 °C at a rate of 10 °C min^{-1}. The thermal gravimetric analyses (TGA) were carried out at a heating of 30 °C to 900 °C with a rate of 20 °C min^{-1} under air flow and registered in a PerkinElmer TGA7 instrument. X-ray Photoelectron spectra (XPS) were recorded using spectrometer model JEOL JPS-9200 (Al Kα, irradiation, $h\nu = 1486.6$ eV, 200 W). The samples under study were supported onto double side conducting copper scotch tape under Ar atmosphere. Binding energy (BE) scale was preliminarily calibrated by the position of the peak Cu 2*p*3/2 (BE = 932.67 eV) core levels. The survey spectra were recorded at pass energy of the analyzer of 50 eV, while that for the narrow spectral regions was 20 eV.

MTA catalytic testing conditions

Zn modified ZSM-5 zeolites were tested as catalysts in the methanol conversion to light aromatics at different reaction temperatures at 400, 425 and 450 °C in a Microactivity reaction set (PID Eng & Tech) consisting of a fixed bed reactor completely automated and controlled from a computer. The reactor outlet is connected to a gas chromatograph to analyze the reaction products. N_2 was used as a stripping gas under a controlled flow. The methanol was fed as a liquid using an HPLC pump (Gilson 307). The methanol was converted to the gas phase and mixed with the N_2 stream in a preheater at 180 °C to generate a gas mixture with a constant molar ratio of methanol/N_2 of 4. Before the reaction, the catalysts were activated at 550 °C for 1 h low air flow to remove any trace of organic molecules or moisture adsorbed within the pores of the catalyst. Typically, the sample was compacted and sieved in a 20–30 mesh, corresponding to a particle size between 0.84 and 0.59 mm. The weight of the catalyst and the flow of methanol were optimized to achieve different values of WHSV (4.74 and 9.48 h^{-1}). The reaction products were analyzed online by gas chromatography with a VARIAN CP3800 chromatograph. The device is equipped with two columns: (i) a Petrocol DH50.2 capillary column connected to an FID detector, and (ii) a Hayesep Q packed column (2 m length, 3.17 mm (1/8″) diameter external and 2 mm internal diameter) connected to a TCD detector, to analyze hydrocarbons and oxygenated products, respectively.

Results and discussion

Catalyst characterizations

Fig. S1 (Supplementary Information) shows the XRD patterns of the H-ZSM-5. All these zeolites exhibit typical diffraction peaks of MFI structure, composed of aggregates of nanosized crystalline units [17]. The characteristic peaks of ZnO at 31.8° and 36.3° were not observed in zeolites with Zn content [18], suggesting that Zn species were highly dispersed on ZSM-5 zeolite after the incorporation of zinc. Almutairi et al. [19] reported that Zn species dispersed on the external surface of ZSM-5 and stabilized at the cation-exchange sites, which could cause lattice distortion of ZSM-5. Hence, Zn species partly interacted with the ZSM-5 framework and influenced the lattice structure of ZSM-5.

Fig. 1a and b shows SEM images of HZ50 0.01 Zn-G and HZ25 zeolites, respectively. It can be seen that the two catalysts present different particle size and morphology. HZ50 0.01 Zn-G image shows spherical particles with a certain roughness of size around 8 µm of diameter (Fig. 1a). As seen in the Fig. 1b, HZ25 zeolite appeared as irregular hexagonal sheets crystal morphology with a mean particle size of more than 2 µm. This type of morphology is referred to as unilamellar [20]. SEM images of nano HZnZ25-i (ratio Si/Al 25) zeolite show spherical and uniform particles (60–80 nm range in diameter), and very rough surface (Fig. S2a). The high magnification SEM image (Fig. S2b) further reveals that they are highly mesoporous, attributed to the agglomerate of nanoparticles of 60–80 nm. The different morphologies of obtained zeolites were caused to a large extent by synthesis conditions even when the same template was used.

The TEM images in Fig. 2 the formation of nanocrystals is clearly observed (ca. 60–80 nm range), and no chunks of Zn specials can be observed on the external surface of the zeolite crystals in each sample. This could be due to the incorporation of Zn into the zeolite framework and the high dispersion of the extra-framework zinc species. This result agrees with the observed in ^{27}Al NMR due to the reduction of the peak assigned to the substitution of Zn by Al extra-framework. The electron

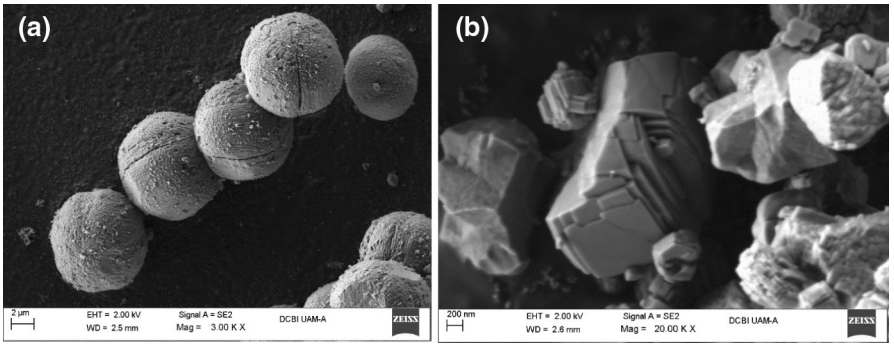

Fig. 1 SEM images of the samples: **a** HZ50 0.01 Zn-G, **b** HZ25 (acid zeolite). The images have a magnification of 3000 and 20,000, respectively

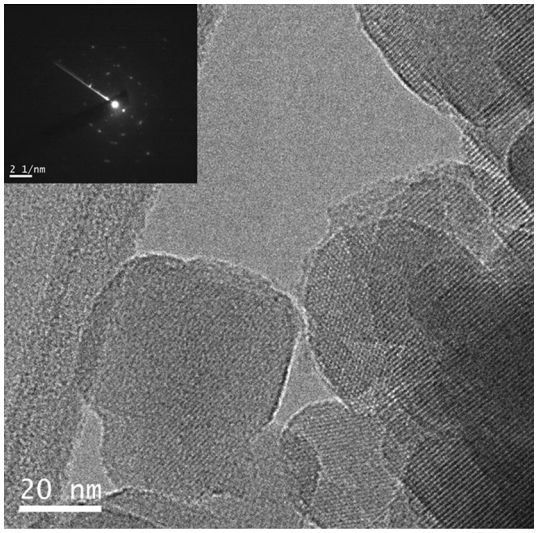

Fig. 2 TEM image of the samples of nano HZnZ25-i. One sets of particles population is detected in the range 60 to 80 nm

diffraction spot pattern of a selected area in HRTEM image (inset of Fig. 2) evidences this fact. Other SEM figures show in Fig. S3 in Supplementary Material. The jointed nanocrystals create many inter-lattice mesopores in zeolite crystalline frameworks (Fig. S3b, c). Smaller zeolite crystals should favor these reactions as the number of pore mouths (active sites) is increased.

On the one hand, the thermal gravimetric analyses (TGA) and derivate thermal gravimetric (DTG) curves of ZSM-5 zeolites uncalcined are shown in Figs. S4 and S5, respectively (Supplementary Information, Figs. S4 and S5). Samples prior to calcination show three weight loss (Fig. S4). The first mass loss to lower than 100 °C, correspond to adsorption water retained in the samples. The weight loss that appears between 450 and 550 °C was due to oxidative decomposition of structure directing agent (SDA). The loss of organic deposited on nano-Z5 sample (9.84%) was lower than that on the hydrothermal ZSM-5 (10.81%) and modified Z50 0.01 Zn-G (10.2%) samples, and the decomposition temperature for nano-Z5 (uncalcined) sample was higher than those on the two other catalysts, which indicated that the organic species (TPABr and TPAOH) within the channels of the nanocrystals were eliminated [21]. On the other hand, in Fig. S5a and b, the curves ATG and ATD, respectively of zeolites ZSM-5 after calcining, are shown. A single loss of mass less than 100 °C is observed, which corresponds to the physisorption of water retained in the samples. No other significant weight losses are observed at higher temperature which indicates that the SDA was eliminated.

Fig. S6 (Supplementary Material) presents the N_2 adsorption–desorption isotherms of the as prepared HZSM-5 samples. Curves a, b and c show isotherms prepared by conventional hydrothermal synthesis, these zeolites show a typical type-I isotherm, according to the IUPAC, which is usually observed for microporous materials having relatively low external surfaces [22]. The N_2 adsorption–desorption isotherm of each catalyst showed a steep increase at low relative

pressure region (P/Po < 0.1) due to the presence of micropores [23] and a long plateau at high relative pressures (0.4 < P/Po < 0.9), indicating that the material is a purely microporous phase with negligible mesoporosity [24]. Nano-ZSM-5 zeolite samples exhibit features of both type I profiles with a high amount adsorbed at 0.45 < P/Po < 0.90 locations (Fig. 2d, e), responding for micropore filling and mesopore capillary condensation [22]. In addition, similar the isotherms of the previous samples these samples exhibit a H4-shaped hysteresis, which is caused by capillary condensation during adsorption, which is attributed to its agglomerate morphology of nanocrystals of 60–80 nm range [25]. This finding is in accordance with SEM images obtained from the same sample.

The surface area and micropore volume of these zeolites are listed in Table 1, which were calculated using the BET equation and t-plot method, respectively. The materials synthesized by the conventional method (without sonication) show the lowest BET surface area, which may be assigned to physicochemical properties of the starting materials and the synthesis method. The nano HZnZ25-i zeolite had a much higher BET area and a larger microporous volume (468 $m^2\ g^{-1}$ and 0.123 $cm^3\ g^{-1}$, respectively) compared to HZnZ25-i zeolite (369 $m^2\ g^{-1}$ and 0.144 $cm^3\ g^{-1}$). Similarly, the nano HZ25 sample showed a larger specific area (428 $m^2\ g^{-1}$) compared to the sample synthesized by the hydrothermal method (428 $m^2\ g^{-1}$) due to the presence of smaller crystals. indicating the Zn species were loaded on the external surface and into the channels of Zn modified HZSM-5 simultaneously [25, 26]. The large surface area is the result of a purely microporous framework with molecular dimensions for shape selectivity which is a characteristic of zeolites. A large external surface area produces to number of pore mouths and increase the accessibility of acid sites in the micropores, which delay the deactivation by coke formation [15].

The amount of Si, Al and Zn in the ZSM-5 zeolites of the calcined samples were determined by ICP-OES analysis (Table 2). It is observed that the incorporation of Zn is efficient both by ion exchange and in the synthesis gel. The acid nanocrystalline zeolite exchanged with zinc had the highest Zn concentration (1.1 wt%). The relation Si/Al to real was measured in all the catalysts, being less than the theoretical in all cases with relatively low Zn/Al ratios. The Si/Al ratio was reproducible through multiple repeats of our synthetic procedure indicating

Table 1 Textural properties of zinc-containing ZSM-5 zeolites prepared

Catalyst	S_{BET} ($m^2\ g^{-1}$)	S_{micro} ($m^2\ g^{-1}$)	$S_{external}$* ($m^2\ g^{-1}$)	V_{micro} ($cm^3\ g^{-1}$)
Nano HZnZ25-i	468	350	118	0.123
Nano HZ25	428	350	78	0.135
HZnZ25-i	369	293	76	0.114
HZ25	403	247	156	0.101
HZ50 0.01 Zn-G	339	250	89	0.124

*Calculated by t-plot method

Table 2 Chemical composition (wt%) determined by ICP-OES of samples

Catalyst	Theoretical molar ratio Si/Al	Si wt%	Al wt%	Real molar ratio Si/Al	Zn wt%	Ratio Zn/Al
Nano HZnZ25-i	25	38.46	1.80	20.53	1.1	2.52
Nano HZ25	25	34.37	2.04	16.21	0.0	–
HZnZ25-i	25	35.98	1.08	21.94	0.88	0.34
HZ25	25	36.15	1.64	20.88	0.0	–
HZ50 0.01 Zn-G	50	36.09	0.76	45.73	1.08	0.59

that the Al atoms in the synthetic solutions w ere incorporated into the framework structures of the ZSM-5 zeolites during the hydrothermal synthesis.

The acid properties of catalysts were determined by NH_3-TPD technique, as presented in Fig. 3. The spectra of all samples exhibit two peaks characteristic throughout the temperature range in all zeolites. The low-temperature (LT) region of 200–300 °C and the high temperature (HT) region of 400–500 °C, which are attributed to the NH_3 adsorbed on the acidic hydroxide group Si–OH–Al [27]. The LT peak is assigned to the weakly held ammonia adsorbed on acid sites to the zeolite [26–28]. The weak adsorption sites of ammonia are inactive in MTA reactions [29]. On the other hand, the HT peak above 400 °C is due to the desorption of NH_3 from strong acid sites. The incorporation of zinc species on HZSM-5 exhibits a significant influence on the distribution of strong acid sites. It is clearly observed, the intensity of HT peak increased by Zn loading because of the exchange of H^+ with Zn^{2+}, indicating the interaction between the Zn^{2+} ions and Bronsted acid sites on Zn-modified ZSM-5 zeolites giving cationic species of Zn, which coordinated with the oxygen atoms in the pore channel [30]. So, the density of the electron cloud in the zeolite framework increased, stronger acidity of the acidic center appeared [31]. These Zn

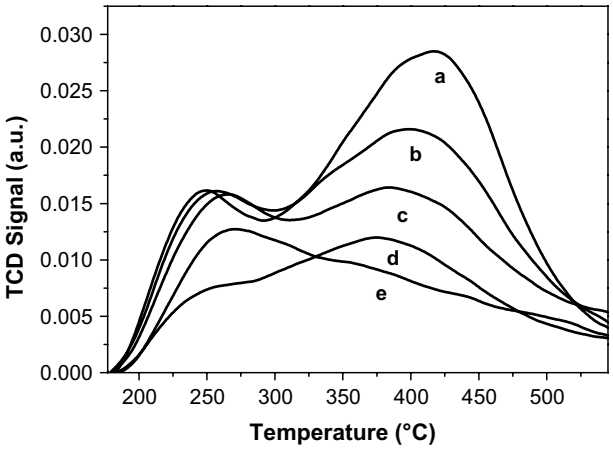

Fig. 3 NH_3-TPD profiles of the parent HZSM-5 zeolites (a) HZnZ25-i, (b) nano HZnZ25-i, (c) nano HZ25, (d) HZ25 and (e) HZ50 0.01 Zn-G

Table 3 Acidity properties of materials

Catalyst	Acidity (mmol NH_3 g^{-1})		
	Weak acid (LT)	Strong acid (HT)	Total
Nano HZnZ25-i	2.634	6.081	8.715
Nano HZ25	–	6.625	6.625
HZnZ25-i	4.967	7.366	12.333
HZ25	1.748	4.610	6.358
HZ50 0.01 Zn-G	7.860	–	7.860

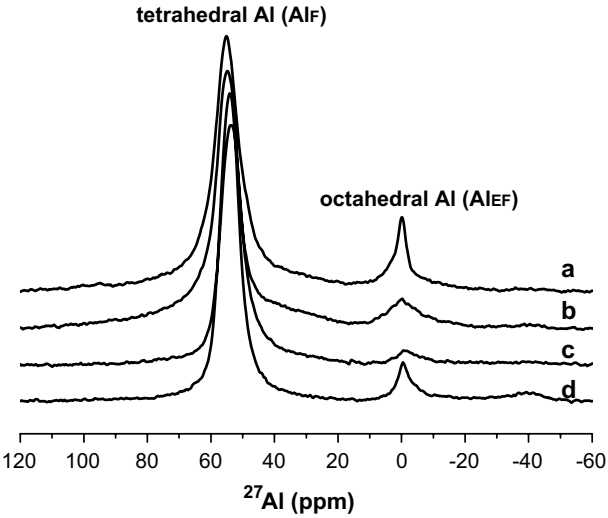

Fig. 4 ^{27}Al MAS NMR spectra of HZSM-5 materials (a) HZ25, (b) HZnZ25-i, (c) nano HZnZ25-i and (d) nano HZ25

sites ($ZnOH^+$) can performance as strong sites to catalyze the reaction and obtain high aromatic selectivity. Traditionally, the HT peak is attributed to NH_3 desorption from strong Brønsted and Lewis acid sites, which are associated with the FAl (framework Al) atoms and are of catalytic importance [32]. The specific peak area is proportional to the number of acid sites in the sample and can be determined by integration by convolution of the area under the curve of the spectra. The amounts of strong and weak acid sites are listed in Table 3. It can be seen that the total concentration of the catalyst hardly exhibited an obvious change with the introduction of Zn.

^{27}Al and ^{29}Si MAS NMR measurements were performed to investigate the different environments of the corresponding atom. The ^{27}Al MAS NMR spectra of all the samples are showed in Fig. 4. Two peaks at 54 ppm and 0 ppm, corresponding to tetrahedral Al (Al_F) entering the zeolite framework and extra-framework octahedral Al atoms (Al_{EF}), respectively. The signal at 0 ppm are ascribed to extra-framework aluminum from either cationic aluminum hydroxide species/hydroxylated alumina-like

clusters inside the channel structure or as framework defects, where hydroxyl groups and water are partly bonded [17, 33]. However, the peak intensity of Al_{EF} decreases slightly due incorporation of Zn in the HZnZ25-i zeolite (Fig. 4b). This indicates AL_{EF} sites are incorporated into the framework structure and that defect sites are annealed by the ion exchange treatment, since the amounts of octahedral Al is reduced [17]. This observation is also occurred in Fig. 4c where is observed that after the incorporation of Zn in the nanocrystalline zeolite (nano HZnZ25-i) the amounts of Al(V) and Al(VI) are reduced after the ion exchange treatment due Al_{EF} is incorporated into the framework after calcination at 550 °C. This result explains the excellent catalytic activity of nano catalyst HZnZ25-i by presenting a greater distribution of strong acid sites in comparison with the zeolite acid nano HZ25.

The ^{29}Si MAS NMR spectra (Fig. 5) were provides information about silicon atoms with different bonding environments in the zeolite framework with silicon atoms connected to silicon, aluminum, or other atoms via oxygen bridge [20]. The deconvolution of ^{29}Si spectrum may result in two peaks centered. The resonances between − 112 and − 115 ppm due to its amorphous state with silicon atoms connected with multiple hydroxyl groups Si (4Si, 0Al). The two bands around − 105 and − 109 ppm correspond to Si (3Si, 1Al) sites or $(AlO)Si(OSi)_3$, that is, Si atoms with one neighboring Al atom [34, 35]. That last signal of the nano HZn25-i samples decreased with the Zn content, which indicated that Zn atom was easier to incorporate into the framework of the ZSM-5 zeolite and resulted in the larger amount of Brønsted acid sites formed by $(ZnO)Si(OSi)_3$ or $(AlO)\ Si(OSi)_3$ [27], indicating that Zn is incorporated in the structure mainly over the Brønsted sites.

Fig. S7 (Supplementary Material Fig. S7) presents Zn 2*p*3/2 core-level spectra obtained for samples. Depending on the preparation method, the distinct variation of the XPS spectra in shape and position demonstrates that the preparation method for introducing zinc species has a significant influence on the existent state of the

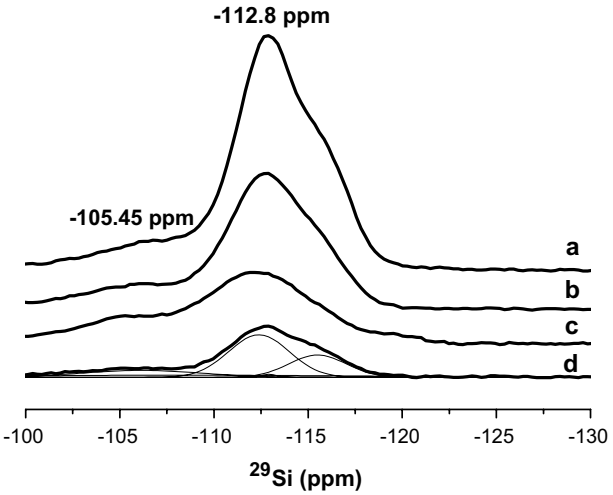

Fig. 5 ^{29}Si MAS NMR spectra of (a) HZ25, (b) HZnZ25-i, (c) nano HZnZ25-i and (d) nano HZ25

surface zinc species. In the case of HZ50 0.01 Zn-G sample shows a Zn 2*p*3/2 peak at 1022.1 eV represents the formation of Zn–O bonds [20]. In the case of HZnZ25-i, the Zn 2*p*3/2 peak is shifted towards higher binding energies (around 1024.28 eV) suggest the presence of the zinc species having tighter interaction with the parent zeolite framework. This can be reasonably assigned to Zn^{2+} cations in the cation exchanged sites of HZnZ25-i zeolite. Chen et al. attributed the high binding energy peak to $ZnOH^{+}$ species [36], which is formed from the strong interaction between the zinc species and the protonic acid sites. On the other hand, Tamiyakul et al. [37] have concluded that the Zn species localized at the ionic exchanged sites show a high binding energy of about 1024 eV because the lattice oxygen of the zeolite exhibits higher electronegativity than the O^{2-} ligand in bulk zinc oxide.

Catalytic evaluation

The catalytic performances of HZSM-5 and Zn-modified HZSM-5 in MTA reaction in 1 h of reaction and WHSV of 9.48 h^{-1} were listed in Table 4. The introduction of zinc species as well as the synthesis method exhibits a significant influence on the catalyst lifetime, methanol conversion, and product distribution. As reported by Jia et al. [38], acid species Lewis type ($^{+}Z–O\cdots H\cdots O–Zn^{2+}$) are able to activate dehydroaromatization of methanol by exchange of Zn in an acid zeolite, which is formed from the strong interaction between the zinc species and the intrinsic acid sites. In 1 h of reaction HZ25 catalyst presented 99.71% methanol conversion, 13.44% BTX selectivity, and HZnZ25-i exhibited 93.60% methanol conversion, with a higher BTX selectivity (21.54%), which indicates that the incorporation of zinc by ion exchange increases the formation of aromatic compounds with the zeolite synthesized by hydrothermal conventional treatment. Acid zeolite HZ25 showed high selectivity towards light olefins C_2–C_4 (48.41%). Dyballa et al. [39] demonstrated that HZSM-5 zeolite exhibits high selectivity to olefins in the reaction of methanol

Table 4 Distribution of reaction products of Zn-modified HZSM-5 (Al/Si 15 ratio) catalysts in the conversion of methanol

Catalyst	HZ25	HZnZ25-i	Nano HZ25	Nano HZnZ25-i
Crystal size	2 µm	2 µm	80 nm	80 nm
Methanol conversion (%)	99.71	93.6	99.88	97.42
Selectivity to products (% mol)				
Olefins C_2–C_4	48.41	38.39	36.69	38.33
Paraffins + olefins C_5^{+}	27.85	19.76	25.46	15.93
Bencene	0.43	0.45	0.88	1.25
Toluene	2.66	3.91	4.91	8.74
Xilenes	10.31	17.18	14.65	19.59
C_9–C_{12}	10.35	20.30	17.41	16.16
BTX total	13.44	21.54	20.44	29.58

Conditions: TOS 1 h, WHSV 9.48 h^{-1}, 450 °C

to olefins (MTO). They indicate that the formation of olefins depends significantly on the presence of a high density of Bronsted acid sites.

On the other hand, nano HZ25 catalyst shows 99.88% methanol conversion and 20.44% BTX selectivity, however, the nano catalyst HZnZ25-i exchanged with Zn with a crystal size in the 60–80 nm range, showed a higher BTX selectivity with a methanol conversion at 1 h of reaction. We demonstrated that activity of Zn-modified zeolites in the MTA reaction with the Zn/ZSM-5 zeolite prepared by ion exchange and demonstrated significantly higher selectivity for aromatics compared with acid ZSM-5 zeolite [40, 41]. The generation of nanocrystalline zeolites influences the optimization of the acid properties of ZSM-5 zeolite to enhance the catalytic activity [15]. The contribution of strong acid sites on the external surface of nano-ZSM-5 are significantly responsible of high shape-selectivity transformation [42]. It was shown that the zeolite with a crystal size in the 60–80 nm range (nano HZnZ25-i) showed better catalytic activity. Konno et al. [43] showed that the generation of nano-sized ZSM-5 zeolites with shorter diffusion length favoured the adsorption and desorption of reactants in the micropores compared with the micro-sized zeolite (2 μm), the MTA activity increased with the decrease of crystal size. Moreover, the selectivity aromatics with large molecular size (C_9–C_{12}) over nano HZnZ25-i was lower than that over HZnZ25-i. These are attributed to the external surface and the excellent porous shape-selectivity of nanocrystalline zeolites [25]. Similarly, Rownaghi and Hedlund [42] reported that nano zeolite displayed more improved BTX yield and catalytic stability than the conventional one, mainly because of reduction of the micropore diffusion path length and an increase of the external surface area by decreasing the zeolite crystal size. On the other hand, the improved selectivity of BTX for nano zeolite should mainly be due to the smaller crystal species which made the acid sites more accessible for reactant [44]. As a result, the oligomerization, cyclization and hydrogen transfer steps occurred easily in MTA reaction which were related closely related to the amount and distribution of both Brønsted acid sites and Lewis acid sites [45, 46].

Effect of temperature on the MTA reaction

Fig. S8a and b show the effects of the reaction temperature on the reactivity of nano HZnZ25-i with a WHSV 9.48 h^{-1}. Fig. 5a shows that the methanol was nearly completely converted to 400 and 425 °C until 3 h of reaction. The conversion of methanol drops to 18% after 9 h of reaction to 450 °C, however, BTX selectivity increased to short reaction times (32%) and subsequently decreased after 7 h to reaction. It is observed that the temperature affects the useful life of the catalyst, as the reaction temperature increases the catalyst tends to deactivate. On the other hand, with an increase of the reaction temperature, the selectivity to BTX increased (Fig. S8b). This indicates that the cokes on the nano HZnZ25-i probably do not cover the active sites and the channels for the reactants and BTX products are not blocked to a low temperature. In addition to temperature, particle size and particle density and kind of active sites on the crystallite surface will be of influence on catalyst lifetime [47, 48].

BTX selectivity increased with a higher contact time (WHSV 4.74 h^{-1}), corresponding to a methanol flux of 50 µm min^{-1} and a catalyst mass of 0.5 g. At 400 and 425 °C, the conversion of methanol is maintained around at 100% during the 9 h reaction (Fig. 6a). After 9 h of reaction the conversion of methanol drops to 84% at a temperature of 450 °C. With these conditions, the best BTX selectivity values are obtained at 450 °C, at short reaction times the selectivity is 32.6% and it drops to 25.4% at 9 h of reaction. At 400 and 425 °C the selectivity remained constant throughout the reaction time around 24 and 28%, respectively (Fig. 6b). These results suggest that an increase in the reaction temperature, specifically at 450 °C, favored the aromatization of methanol, however, to higher reaction temperature suppressed dehydrocyclization and promoted the formation of coke from a secondary reaction [47]. Hence, the BTX yield in MTA process was closely related to the acid amounts [45]. According to other works, these results of total aromatic selectivity (45.76%) are higher compared to those reported by other authors such as Niu et al. [49] and Bi [12], in addition to our catalysts have better lifetime because we obtained shorter crystals size. Likewise, the BET area of our nano HZSM-5 catalysts were larger (400 m^2 g^{-1}) compared to other publications [16] where they synthesized ZSM-5 zeolites of nanocrystalline size.

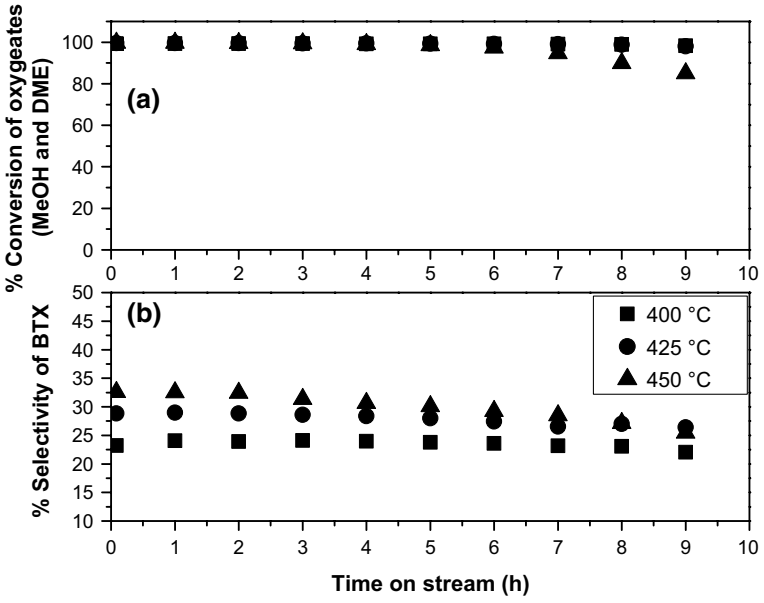

Fig. 6 **a** % Conversion of oxygenates compounds (MeOH and DME) and **b** % selectivity to BTX fraction over nano HZnZ25-i catalyst with WHSV of 4.74 h^{-1}, 0.5 g of catalyst and different temperatures 400 °C (filled square), 425 °C (filled circle) and 450 °C (filled triangle)

Effect of the Zn incorporation form on the zeolites in the MTA reaction

The incorporation of zinc species by ion exchanging (HZnZ25-i) and synthesis gel (HZ50 0.01 Zn-G) has high influence on the catalytic stability methanol conversion, and products distribution to 450 °C (Fig. 7a, b). Zn improved the formation of BTX aromatics in zeolite HZnZ25-i compared to pure acid zeolite HZ25. The enhanced aromatics formation observed for Zn would be the result of metal with the acid sites of the zeolites. It was observed that the reduction of the crystal size in the nanocrystalline zeolites improved the interaction of Zn with the acidity of the ZSM-5 zeolite, improving diffusion processes by physical transport [12], which can dramatically increase the number of pore mouths and increase the accessibility of acid sites in the micropores. These results validated that the strong acid sites in a large amount in the core of the catalyst is crucial for the aromatic selectivity. Their catalytic activities were promoted with the increasing of mesopores and a smaller crystal size, which improving the diffusion efficiency and accessibility of acid sites for high selectivity BTX fraction. In this sense, nano HZ25 and nano HZnZ25-i catalyst show the longest lifetime to 9 h due to the coordination of proportion between Lewis acid sites and Brønsted acid sites and proper pore structure [47].

However, HZnZ50 0.01 Zn-G zeolite shows little stability, the lifetime is decreased to 2 h. This be ascribed to the accumulation of a small amount of nanometric ZnO clusters in the channels of HZ50 0.01 Zn-G zeolite, which avoid to the aromatics diffusion and may accelerate the catalyst deactivation due to coke deposition. Recently, Kim et al. [50] found coke was deposited on the external surfaces

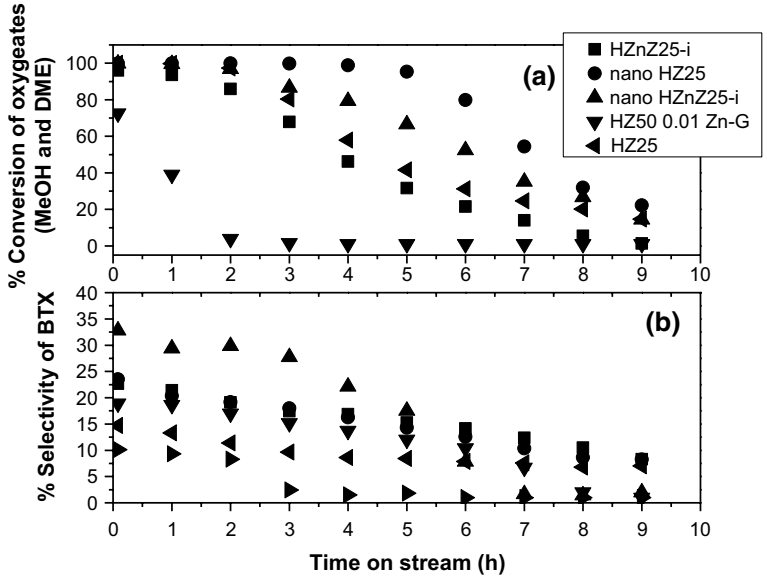

Fig. 7 Results of catalytic activity of MTA reaction over HZSM-5 catalyst with different forms of zinc incorporation **a** conversion of oxygenates compounds (MeOH and DME), **b** selectivity to BTX fraction. Conditions reaction: WHSV of 9.48 h^{-1}, 450 °C, 0.25 g of catalyst

more than it was inside the micropores in the MTA reaction. The stability of catalysts decreases in the sequence of nano HZ25 > nano HZnZ25-i > HZ25 > HZnZ25-i > HZ50 0.01 Zn-G to 450 °C. Some authors [6, 37, 39, 51–53] suggest that the incorporation of Zn by ion exchange method can be three types of Zn species; (i) isolated Zn^{2+} ions stabilized at the cation-exchange sites of the zeolite, (ii) clusters resulting from the condensation of partially hydrolyzed $ZnOH^{+}$ extraframework cations, and (iii) more bulky intrazeolite or extrazeolite clusters of zinc oxide, which incorporated in the acid zeolite are responsible for the catalytic activation at temperatures between 400 and 500 °C. However, it is not known for sure which of the three species are responsible for perform methanol activation.

In other hand, it is clear that the stability increased at a temperature of 400 °C (Fig. S9a, b). The conversion of methanol is maintained around 100% in all the catalysts throughout the entire reaction process, except for the sample HZ50 0.01 Zn-G, the catalyst is deactivated after 8 h of reaction due to coke formation.

In this case, deactivation is usually associated with diffusion limitations of heavy products by the formation of large Zn species formed in the micropores [13, 38], this phenomenon indicates that the inactivation of aromatization reaction is mainly due to the decrease of strong acid sites and the cokes molecules covered that sites. In our work, improved aromatization of methanol results were observed when converting methanol using ZSM-5 zeolite Zn-modified compared to other metals previously studied by other authors. Ag-ZSM-5 [7], Ag/HZSM-5 [54], Cu/Zn/HZSM-5 [55, 56], Mo_2C/ZSM-5 [8], Ga_2O_3/HZSM-5 [57] and H-Ga-ZSM-5 (by exchange) [58] all gave good MTA ability but the BTX selectivity less than those obtained by us.

Conclusions

The catalytic activity of Zn modified ZSM-5 catalysts was studied in methanol conversion to aromatics (MTA). The Zn incorporation method had obvious influences on the textural properties, morphology, acidic properties and catalytic performances. The BTX selectivity was effectively improved by introduction of Zn species by ion exchange, due to a greater distribution of strong acid sites, and the generation of strong acid sites, and these acidic sites are the active sites which are the main responsible of the methanol conversion to aromatics. The reaction temperature is an important variable in the MTA process. At 450 °C a better activation of acid sites is achieved in zeolite with Zn and therefore a high percentage of BTX selectivity is obtained.

The combination of physical characteristics such as very small crystal size, high external surface area, and strong acidity makes uniform nano ZSM-5 a potentially interesting catalyst in MTA processes. The generation of nanocrystallites of approximately in the 60–80 nm range in the nano zeolite HZnZ25-i drastically improved the catalytic activity. Nano zeolite increased the diffusion efficiency of molecules and the accessibility of acid sites, improving the BTX selectivity. Under the optimal conditions 450 °C and WHSV 4.74 h^{-1}, 0.5 g of catalyst and 50 µm min^{-1} of methanol nearly 100% methanol conversion and 32.5% selectivity BTX (with 9 h lifetime) was obtained. The temperature reaction has great influence on the catalytic activity,

at 450 °C the best BTX selectivity is obtained, however, the catalyst is deactivated after 9 h of reaction. The stability of catalysts decreases in the sequence of nano HZ25 > nano HZnZ25-i > HZ25 > HZnZ25-i > HZ50 0.01 Zn-G to 450 °C and WHSV of 9.48 h^{-1}. Deactivation of catalyst is due of a small amount of ZnO clusters in the channels of HZSM-5 zeolite, which avoid to the aromatics diffusion and may accelerate the catalyst deactivation due to coke deposition that block the acid sites of the zeolite. Coke deposition was known to be the major reason for catalyst deactivation in MTA reaction.

Acknowledgements The authors thank the Spanish Research Agency-AEI and the European Regional Development Fund-FEDER for the financing of this work, through the Project MAT2016-77496-R (AEI/FEDER, EU), MGR thanks the Molecular Sieve Group of the Institute of Catalysis and Petrochemistry (CSIC) in Madrid and CONACyT for the support granted for the research stay in Spain

References

1. Fahim M, Alsahhaf T, Elkilani A (2010) Fundamentals of petroleum refining, 1st edn. Elsevier Science, Kuwait
2. Wang N, Qian W, Shen K, Su C, Wei F (2014) Bayberry-like ZnO/MFI zeolite as high performance methanol-to-aromatics catalyst. Ind Eng Chem Res 53:14932–14940
3. Conte M, Lopez-Sanchez JA, He Q, Morgan DJ, Ryabenkova Y, Bartley JK, Carley AF, Taylor SH, Kiely CJ, Khalid K, Hutchings GJ (2012) Modified zeolite ZSM-5 for the methanol to aromatics reaction. Catal Sci Technol 2:105–112
4. Zhu X (2015) Hierarchical zeolites as catalysts for methanol conversion reactions. Technische Universiteit Eindhoven, Eindhoven
5. Haw JF, Song W, Marcus DM, Nicholas JB (2003) The mechanism of methanol to hydrocarbon catalysis. Acc Chem Res 36:317–326
6. Zhang GQ, Bai T, Chen TF, Fan WT, Zhang X (2014) Conversion of methanol to light aromatics on Zn-modified nano-HZSM-5 zeolite catalysts. Ind Eng Chem Res 53:14932–14940
7. Inoue Y, Nakashiro K, Ono Y (1995) Selective conversion of methanol into aromatic hydrocarbons over silver-exchanged ZSM-5 zeolites. Microporous Mater 4(379):383
8. Barthos R, Bánsági T, Zakar TS, Solymosi F (2007) Aromatization of methanol and methylation of benzene over Mo_2C/ZSM-5 catalysts. J Catal 247:368–378
9. Yubing X, Puyu Q, Xinping D, Haiqiang L, Youzhu Y (2013) Enhanced performance of Zn–Sn/HZSM-5 catalyst for the conversion of methanol to aromatics. Catal Lett 143:798–806
10. Zhou F, Gao Y, Ma H, Wu G, Liu C (2017) Catalytic aromatization of methanol over post-treated ZSM-5 zeolites in the terms of pore structure and acid sites properties. Mol Catal 438:37–46
11. Ni Y, Sun A, Xi Wu, Hai G, Hu J, Li T, Li G (2011) The preparation of nano-sized H[Zn, Al] ZSM-5 zeolite and its application in the aromatization of methanol. Microporous Mesoporous Mater 143:435–442
12. Bi Y, Wang Y, Chen X, Yu Z, Xu L (2014) Methanol aromatization over HZSM-5 catalysts modified with different zinc salts. Chin J Catal 35:1740–1751
13. Gabrienko AA, Arzumanov SS, Toktarev AV, Danilova IG, Prosvirin IP, Kriventsov VV, Zaikovskii VI, Freude D, Stepanov AG (2017) Different efficiency of Zn^{2+} and ZnO species for methane activation on Zn-modified zeolite. ACS Catal 7:1818–1830
14. Pan D, Song X, Yang X, Gao L, Wei R, Zhang J, Xiao G (2018) Efficient and selective conversion of methanol to para-xylene over stable H[Zn, Al]ZSM-5/SiO_2 composite catalyst. Appl Catal A 557:15–24
15. Ji Y, Yang H, Yan W (2017) Strategies to enhance the catalytic performance of ZSM-5 zeolite in hydrocarbon cracking: a review. Catalysts 7(367):1–31
16. Petushkov A, Yoon S, Larsen SC (2011) Synthesis of hierarchical nanocrystalline ZSM-5 with controlled particle size and mesoporosity. Microporous Mesoporous Mater 137:92–100

17. Pinilla-Herrero I, Borfecchia E, Holzinger J, Mentz UV, Finn J, Lomachenko KA, Bordiga S, Lamberti C, Berlier G, Olsbye U, Svelle S, Skibsted J, Beato P (2018) High Zn/Al ratios enhance dehydrogenation vs hydrogen transfer reactions of Zn-ZSM-5 catalytic systems in methanol conversion to aromatics. J Catal 362:146–163
18. Tian ZR, Voigt JA, Liu J, Mckenzie B, Mcdermott MJ, Rodriguez MA, Konishi H, Xu H (2003) Complex and oriented ZnO nanostructures. Nat Mater 2:821–826
19. Almutairi SM, Mezari B, Magusin PC, Pidko EA, Hensen EJ (2012) Structure and reactivity of Zn-modified ZSM-5 zeolites: the importance of clustered cationic Zn complexes. ACS Catal 2:71–83
20. Wang Y, Song J, Baxter NC, Kuo GT, Wang S (2017) Synthesis of hierarchical ZSM-5 zeolites by solid-state crystallization and their catalytic properties. J Catal 349:53–65
21. Jin F, Wang X, Liu T, Xiao L, Yuan M, Fan Y (2017) Synthesis of ZSM-5 with the silica source from industrial hexafluorosilicic acid as transalkylation catalyst. Chin J Chem Eng 25:1303–1313
22. Thommes M, Kaneko K, Neimark A, Olivier J, Rodriguez-Reinoso F, Rouquerol J, Sing K (2015) Physisorption of gases, with special reference to the evaluation of surface area and pore size distribution (IUPAC technical report). Pure Appl Chem 87:1051–1069
23. van Laak AN, Sagala SL, Zecevic J, Friedrich H, de Jongh PE, de Jong KP (2010) Mesoporous mordenites obtained by sequential acid and alkaline treatments: catalysts for cumene production with enhanced accessibility. J Catal 276:170–180
24. Fang Y, Su X, Bai X, Wu W, Wang G, Xiao L, Yu A (2017) Aromatization over nanosized Ga-containing ZSM-5 zeolites prepared by different methods: effect of acidity of active Ga species on the catalytic performance. J Energy Chem 26:768–775
25. Li J, Tong K, Xi Z, Yuan Y, Hu Z, Zhu Z (2016) High-efficient conversion of methanol to p-xylene over shape-selective Mg-Zn-Si-HZSM-5 catalyst with fine modification of pore-opening and acidic properties. Catal Sci Technol 6(13):4802–4813
26. Zhang J, Qian W, Kong C, Wei F (2015) Increasing para-xylene selectivity in making aromatics from methanol with a surface-modified Zn/P/ZSM-5 catalyst. ACS Catal 5:2982–2988
27. Su X, Wang G, Bai X, Wu W, Xiao L, Fang Y, Zhang J (2016) Synthesis of nanosized HZSM-5 zeolites isomorphously substituted by gallium and their catalytic performance in the aromatization. Chem Eng J 293:365–375
28. Jia Y, Wang J, Zhang K, Chen G, Yang Y, Liu S, Ding C, Meng Y, Liu P (2018) Hierarchical ZSM-5 zeolite synthesized via dry gel conversion-steam assisted crystallization process and its application in aromatization of methanol. Powder Technol 328:415–429
29. Topsøe N, Pedersen K, Derouane E (1981) Infrared and temperature-programmed desorption study of the acidic properties of ZSM-5-type zeolites. J Catal 70:41–52
30. Joly JF, Ajot H, Merlen E, Raatz F, Alario F (1991) Parameters affecting the dispersion of the gallium phase of gallium H-MFI aromatization catalysts. Appl Catal A 79:249–263
31. Xiaoning W, Zhen Z, Li Z, Guiyuan J (2007) Effects of fight rare earth on acidity and catalytic performance of HZSM-5 zeolite for catalytic clacking of butane to light olefins. J Rare Earths 25:321–328
32. Reddy JK, Motokura K, Koyama T, Miyaji A, Baba T (2012) Effect of morphology and particle size of ZSM-5 on catalytic performance for ethylene conversion and heptane cracking. J Catal 289:53–61
33. Saito H, Inagaki S, Kojima K, Han Q, Yabe T, Ogo S, Kubota Y, Sekine Y (2018) Preferential dealumination of Zn/H-ZSM-5 and its high and stable activity for ethane dehydroaromatization. Appl Catal A 549:76–81
34. Iwase Y, Motokura K, Koyama T, Miyaji A, Baba T (2009) Influence of Si distribution in framework of SAPO-34 and its particle size on propylene selectivity and production rate for conversion of ethylene to propylene. Phys Chem Chem Phys 11:9268–9277
35. Jakkidi K, Motokura K, Koyama T, Miyaji A, Baba T (2012) Effect of morphology and particle size of ZSM-5 on catalytic performance for ethylene conversion and heptane cracking. J Catal 289:53–61
36. Chen J, Feng Z, Ying P, Li C (2004) ZnO clusters encapsulated inside micropores of zeolites studied by UV Raman and laser-induced luminescence spectroscopies. J Phys Chem B 108(34):12669–12676
37. Tamiyakul S, Ubolcharoen W, Tungasmita DN, Jongpatiwut S (2015) Conversion of glycerol to aromatic hydrocarbons over Zn-promoted HZSM-5 catalysts. Catal Today 256:325–335
38. Jia Y, Wang J, Kan Z, Liu S, Chen G, Yang Y, Ding C, Liu P (2017) Catalytic conversion of methanol to aromatics over nanosized HZSM-5 zeolite modified by $ZnSiF_6{\cdot}6H_2O$. Catal Sci Technol 7:1776–1791

39. Dyballa M, Becker P, Trefz D, Klemm E, Fischer A, Jakob H, Hunger M (2016) Parameters influencing the selectivity to propene in the MTO conversion on 10-ring zeolites: directly synthesized zeolites ZSM5, ZSM-11, and ZSM-22. Appl Catal A 510:233–243
40. Gong T, Qin L, Lu J, Feng H (2016) ZnO modified ZSM-5 and Y zeolites fabricated by atomic layer deposition for propane conversion. Phys Chem Phys 18:601–614
41. Ono Y (1992) Transformation of lower alkanes into aromatic hydrocarbons over ZSM-5 zeolites. Catal Rev Sci Eng 34:179–226
42. Rownaghi A, Hedlund J (2011) Methanol to gasoline-range hydrocarbons: influence of nanocrystal size and mesoporosity on catalytic performance and product distribution of ZSM-5. Ind Eng Chem Res 50:11872–11878
43. Konno H, Tago T, Nakasaka Y, Ohnaka R, Nishimura J, Masuda T (2013) Effectiveness of nanoscale ZSM-5 zeolite and its deactivation mechanism on catalytic cracking of representative hydrocarbons of naphtha. Microporous Mesoporous Mater 175:25–33
44. Zhang G, Bai T, Fei T, Fan W, Zhang X (2014) Conversion of methanol to light aromatics on Zn-modified nano-HZSM-5 zeolite catalysts. Ind Eng Chem Res 53:14932–14940
45. Ningning X, Donghui P, Yuanfeng W, Siquan X, Lijing G, Jin Z, Guomin X (2019) Preparation of nano-sized HZSM-5 zeolite with sodium alginate for glycerol aromatization. React Kinet Mech Catal 127(1):449–467
46. Wan ZJ, Li GK, Wang CF, Yang H, Zhang DK (2018) Relating coke formation and characteristics to deactivation of ZSM-5 zeolite in methanol to gasoline conversion. Appl Catal A 549:141–151
47. Zhao YH, Gao TY, Wang YJ, Zhou YJ, Huang GQ (2018) Zinc supported on alkaline activated HZSM-5 for aromatization reaction. React Kinet Mech Catal 125(2):1085–1098
48. Schulz H (2010) "Coking" of zeolites during methanol conversion: basic reactions of the MTO-, MTP- and MTG processes. Catal Today 154:183–194
49. Niu X, Gao J, Miao Q, Dong M, Wang G, Weibin F, Qin Z, Wang J (2014) Influence of preparation method on the performance of Zn-containing HZSM-5 catalysts in methanol-to-aromatics. Microporous Mesoporous Mater 197:252–261
50. Kim J, Choi M, Ryoo R (2010) Effect of mesoporosity against the deactivation of MFI zeolite catalyst during the methanol-to-hydrocarbon conversion process. J Catal 269:219–228
51. Khatamian M, Alaji Z, Khandar A (2011) Synthesis and characterization of polycrystalline ZnO/HZSM-5 nanocomposites. J Iran Chem Soc 8:44–54
52. Kazansky V, Borovkov V, Serikh A, Van Santen R, Anderson B (2000) Nature of the sites of dissociative adsorption of dihydrogen and light paraffins in ZnHZSM-5 zeolite prepared by incipient wetness impregnation. Catal Lett 66:39–47
53. Olsbye U, Svelle S, Bjørgen M, Beato P, Janssens T, Bordiga S, Lillerud K (2012) Conversion of methanol to hydrocarbons: how zeolite cavity and pore size controls product selectivity. Angew Chem Int Ed 51:2–24
54. Tian T, Qian WZ, Sun YJ, Cui Y, Lu YY, Wei F (2009) Aromatization of methanol on Ag/ZSM-5 catalyst. Modern Chem Ind 29(1):55–58
55. Zaidi HA, Pant KK (2004) Catalytic conversion of methanol to gasoline range hydrocarbons. Catal Today 96(3):155–160
56. Zaidi HA, Pant KK (2008) Activity of oxalic acid treated ZnO/CuO/HZSM-5 catalyst for the transformation of methanol to gasoline range hydrocarbons. Ind Eng Chem Res 47(9):2970–2975
57. Freeman D, Wells RP, Hutchings GJ (2002) Conversion of methanol to hydrocarbons over Ga_2O_3/H-ZSM-5 and Ga_2O_3/WO_3 catalysts. J Catal 205(2):358–365
58. Choudhary VR, Kinage AK (1995) Methanol-to-aromatics conversion over H-gallosilicate (MFI): influence of Si/Ga ratio, degree of H^+ exchange, pretreatment conditions, and poisoning of strong acid sites. Zeolites 15(8):732–738

Affiliations

Misael García Ruiz[1] · Dora A. Solís Casados[2] · Julia Aguilar Pliego[3] · Carlos Márquez Álvarez[4] · Enrique Sastre de Andrés[4] · Diana Sanjurjo Tartalo[4] · Raquel Sainz Vaque[4] · Marisol Grande Casas[4]

✉ Misael García Ruiz
misa_gr@hotmail.com

[1] Doctorado en Ciencia de Materiales de la Facultad de Química, Universidad Autónoma del Estado de México, Paseo Colón Esquina Paseo Tollocan S/N, C.P. 50000 Toluca, Mexico, Mexico

[2] Universidad Autónoma del Estado de México, Centro Conjunto de Investigación en Química Sustentable UAEM-UNAM, Personal Académico Adscrito a la Facultad de Química, UAEMex, Mexico, Mexico

[3] Área de Química Aplicada, Departamento de Ciencias Básicas, UAM-A, San pablo 180, C.P. 02200 Mexico City, Mexico

[4] Instituto de Catálisis y Petroleoquímica, CSIC, C/Marie Curie 2, Campus Cantoblanco, 28049 Madrid, Spain